RSC Sustainability

ROYAL SOCIETY OF CHEMISTRY

PAPER

View Article Online
View Journal | View Issue

Cite this: *RSC Sustainability*, 2026, **4**, 1081

Sustainable glycerol-based reactive diluent alternatives to commercial ethylene glycol diacrylate (EGDA) and 2-hydroxyethyl methacrylate (HEMA) for additive manufacturing

Vojtěch Jašek, *[a] Silvestr Figalla,*[a] Veronika Lavrinčíková[ab] and Radek Přikryl [a]

This work proposes an efficient production route to sustainable reactive diluents based on modified glycerol as an alternative to commercial compounds such as 2-hydroxyethyl methacrylate (HEMA) and ethylene glycol diacrylate (EGDA). The synthesis of methacrylated vegetable oil (MO) was performed through nucleophilic substitution catalyzed by an organic base (triethylamine). Glycerol monomethacrylate (MGLY) and glycerol trimethacrylate (TGLY) were produced by Fischer esterification. The structural cross-analysis included ^{1}H NMR, ESI-MS, and FT-IR. The rheological investigation of systems composed of 75 wt% MO and 25 wt% reactive diluent confirmed the diluting role of MGLY and TGLY. The TGLY-based system exhibited a competitive apparent viscosity at 30 °C ($\eta_{30°C}$ = 590 mPa s) and a flow activation energy (E_a = 48.4 kJ mol^{-1}) comparable to those of commercial HEMA- and EGDA-based precursors. The testing specimens for DMA, TGA, and mechanical analysis were successfully fabricated using an mSLA 3D printer, confirming their utility for additive manufacturing. The TGLY-containing system outperformed all the investigated thermosets in the crosslinking density (ν_e = 15.5 kmol m^{-3}), the storage modulus at 30 °C (E' = 473 MPa), and the tensile and flexural moduli. Based on the results, synthesized compounds improved the rheological, thermo-mechanical, and mechanical properties of MO-based thermosets.

Received 28th November 2025
Accepted 12th January 2026

DOI: 10.1039/d5su00891c

rsc.li/rscsus

Sustainability spotlight

The proposed work introduces glycerol-based reactive diluents as alternatives to fossil-based commercially available compounds, 2-hydroxyethyl methacrylate (HEMA) and ethylene glycol diacrylate (EGDA). The synthesized glycerol monomethacrylate and glycerol trimethacrylate reached conversions above 91% and were characterized by numerous structure-confirming methods (^{1}H NMR, ESI-MS, and FT-IR). Our proposed compounds represent sustainable and environmentally safer reactive precursors with enormous potential in additive technologies such as SLA, MSLA, or DLP 3D printing.

1 Introduction

Reactive diluents play an essential and irreplaceable role in many material-based applications, such as reactive adhesives,[1] coatings,[2] pultrusion technology,[3] dental applications,[4] and additive manufacturing.[5] Their primary purpose lies in decreasing the apparent viscosity of the target working system, usually possessing excessive flow character. The regulation of the rheological profile is directly linked to the essential factors that influence specific applications.[6] Adhesives and coatings demand modifiable viscosity due to the thin-layer fabrication.[7] Pultrusion on composite matrices for dental applications requires optimal compatibility of the resin continuum and the dispersed heterogeneous phase to ensure the best functional performance.[3,4] Additive manufacturing depends enormously on the reached viscosity level of the resin-forming precursor system.[8] The conventional stereolithography (SLA) technology requires a polymerizable system triggered through photo-reactive initiators such as phenylbis(2,4,6-trimethylbenzoyl) phosphineoxide (BAPO) or diphenyl(2,4,6-trimethylbenzoyl) phosphine oxide (TPO).[9] The rheological profile is a critical property since the 3D printing technology relies on the limited resin viscosity (usually up to 5 Pa s).[8] Systems possessing exceptionally high viscosity (typically high molecular weight systems or particular compounds from renewable sources, such as curable vegetable oils) require modification of their flow properties.[10] The non-diluted highly viscous precursors applied in additive manufacturing usually lead to insufficiently detailed and precisely printed prototypes.[11] Next to the SLA 3D printing approach using a single laser as the irradiation source, other

[a]*Institute of Materials Chemistry, Faculty of Chemistry, Brno University of Technology, 612 00 Brno, Czech Republic. E-mail: xcjasekv@vutbr.cz; xcfigallas@vutbr.cz*
[b]*Materials Research Centre, Faculty of Chemistry, Brno University of Technology, 612 00 Brno, Czech Republic*

instrumental compositions (digital light processing (DLP), *etc.*) are included in processes that perform vat-photopolymerization. Generally, vat-photopolymerization methods involve a photo-reactive resin and an appropriate initiator placed in a vat. The particular type of irradiation source selectively triggers the liquid precursor in defined areas and layers, resulting in a 3D-printed object. With each polymerized layer, the 3D printing platform, holding the polymerized resin, moves up by a selected distance.[49]

Fossil-based reactive diluents are widely used to modify rheology in numerous applications.[12] Volatility is one of the most investigated properties of viscosity-modifying compounds. Highly volatile molecules, such as styrene or methyl methacrylate, produce high levels of volatile organic compounds (VOCs); therefore, their use could pose health and environmental hazards.[6] Several petroleum-based reactive diluents were engineered to reduce VOCs, leading to less hazardous compounds, such as ethylene glycol diacrylate (EGDA),[13] ethylene glycol methacrylate (EGDMA),[14] tripropylene glycol diacrylate (TPGDA),[15] 1,6-hexanediol diacrylate (HDDA),[16] 2-hydroxyethyl methacrylate (HEMA),[17] or acryloyl morpholine (ACMO).[18] The main differences are properties such as the mentioned volatility or the polymerization functionality. The more reactive functional groups, the higher the crosslinking density of the eventual thermoset.[6] The modified glycerol derivatives suitable for curable applications were investigated in the literature. Poly(glycerol) acrylate was synthesized *via* a condensation reaction, serving as a 3D-printable reactive precursor with high viscosity (6.5 Pa s).[56] A similar approach was applied in another published article focused on sustainable additive manufacturing.[57] Moreover, maleic anhydride-based glycerol-involving acrylates were proposed and investigated, representing a highly stretchable 3D printed crosslinked resin.[58] On the other hand, methacrylate glycerol derivatives have not yet been reported in the literature.

Nowadays, bio-based alternatives are attracting significant attention due to legislative changes and efforts towards sustainable manufacturing.[19] The statistics of 2024 uncover that aliphatic-based reactive diluents represent 40.24% of the total market, where the bio-based representatives are on track for 6.66% until 2030.[20] Also, the most significant application segment for reactive diluents was paints and coatings (46.45%) by 2024, where 3D printed resins could reach a 6.34% compound annual growth rate (CAGR) through 2030.[20] Numerous commercial bio-based reactive diluents are available on the market, such as isobornyl acrylate (IBOA),[21] isobornyl methacrylate (IBOMA),[22] epoxidized soybean oil (ESO),[6] furfurylglycidyl ether (FGE),[23] or methacrylated eugenol (ME).[24] Although these compounds contain structures from renewable sources, their availability and price are the most challenging factors connected to their utility in the global reactive diluent market.[25] Besides their high cost, several highly reactive and hazardous chemicals are used for their fabrication, such as acyl halides,[26] carboxyl anhydrides,[27] or glycidyl derivatives.[28] The exceptional reactivity of the reactants used increases the expenses and hazardous impact connected to their production.[6]

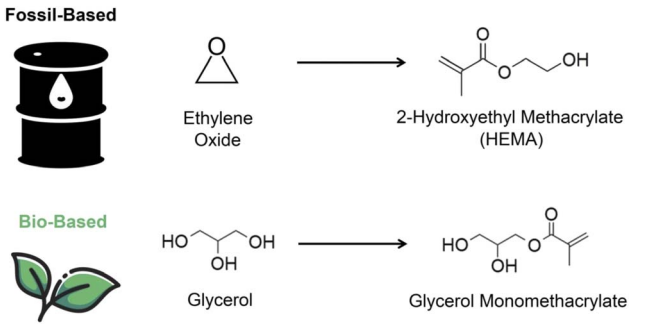

Fig. 1 Two representatives of mono-functional aliphatic reactive diluents – the fossil-based 2-hydroxyethyl methacrylate (HEMA) and bio-based glycerol monomethacrylate (MGLY) compounds investigated in this work.

This work investigates the synthesis, characterization, and application of sustainable compounds derived from glycerol, an available aliphatic starting material. Methacrylic acid, a cheap and less hazardous reactant compared to the commonly used acyl halides or anhydrides, was used to modify glycerol into curable low-viscosity precursors. The main aim of this study is to suggest appropriate alternatives to currently widely used reactive diluents, ethylene glycol diacrylate and 2-hydroxyethyl methacrylate (illustrated in Fig. 1). Next to the selection of available and suitable reactants, the solvent-less synthesis using vacuum distillation was introduced to emphasize the process's scalability, which is linked to the limitation on VOC generation. The synthesized bio-based reactive diluent alternatives, glycerol monomethacrylate (MGLY) and glycerol trimethacrylate (TGLY), were characterized *via* ^{1}H NMR, ESI-MS, and FT-IR analyses. This work also involves the synthesis of methacrylated vegetable oil (MO), a highly viscous, curable precursor suitable for additive manufacturing. This system demonstrated the effects of commercial and synthesized bio-based reactive diluents. We prepared a total of 4 systems containing highly viscous MO diluted with the reference and custom reactive diluents to investigate the rheological profile, thermal stability, thermo-mechanical properties, and tensile/flexural deformation characteristics of the liquid precursors and the 3D-printed test specimens. Eventually, we summarized the positive and negative outcomes of applying commercial and custom-synthesized diluents, as determined by the performed experiments.

2 Experimental section

2.1 Materials

Glycerol (99%), potassium hydroxide (99%), sulfuric acid (98%), sodium sulfate (99%, anhydrous), and ethyl acetate (99%) were purchased from Penta Ltd (Czech Republic). Epoxidized vegetable oil (99%), methacrylic acid (98%, MeQH stabilized), triethylamine (99%) BAPO (photoinitiator, phenylbis(2,4,6-trimethylbenzoyl)phosphine oxide, 98%), d-chloroform (solvent for NMR analyses, $CDCl_3$), 2-hydroxyethyl methacrylate (97%), and ethylene glycol diacrylate (EGDA, 98%) were obtained from Sigma-Aldrich (Merck, Germany).

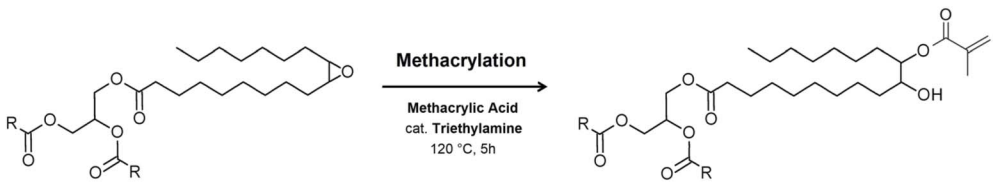

Fig. 2 The reaction scheme of methacrylated vegetable oil synthesis through methacrylation catalyzed by triethylamine.

2.2 Structural verification methods

Acid value (A. V.) quantifies the number of acidic functional groups. The applied norm for the A. V. was ČSN EN ISO 660. The sample size was 100 mg.

Nuclear magnetic resonance (NMR) was applied to obtain ^{1}H spectra to confirm the structural identity of the synthesized compounds. We used a Bruker Avance III 500 MHz (Bruker, Billerica, MA, USA). The measuring frequency was 500 MHz for ^{1}H NMR. The measurements were performed at 30 °C using d-chloroform ($CDCl_3$) as the solvent with tetramethylsilane (TMS) as the internal standard. The sample concentration was 10 mg mL^{-1}. The chemical shifts (δ) are expressed in parts per million (ppm) units, referenced to a solvent. The coupling constant (J) is expressed with the frequency unit (Hz), with coupling expressed as s-singlet, d-doublet, t-triplet, q-quartet, p-quintet, and m-multiplet.

Electrospray mass spectrometry (ESI-MS) contributed to the structural cross-analysis of synthesized compounds. We used a Bruker EVOQ LC-TQ (Bruker, Billerica, MA, USA) instrument for the measurements. Product scan spectra were obtained by fragmentation of the following molecular precursor ions ($[M - H_2O + H]^+$), detailed in the synthesis section for every produced compound. Collision energy spread (5–20 eV) improved the collected MS/MS data quality. Furthermore, the obtained mass spectra agree with their *in silico* predictions by CFM-ID 4.0,[29] which also proposed product-ion structures for the most intense masses. The sample concentration was 10 μg mL^{-1}.

Table 1 The reaction mixture composition for MGLY and TGLY synthesis

Product	Glycerol (g)	Methacrylic acid (g)	Catalyst sulfuric acid (g)
MGLY	92	86	0.98
TGLY	92	258	0.98

Fourier-transform infrared spectroscopy (FT-IR) was used as a structural confirmation method to detect specific functional groups in the synthesized compounds. Analyses were performed using a Bruker Tensor 27 (Billerica, MA, USA) and the attenuated total reflectance (ATR) method. Diamond served as a dispersion component. A diode laser was the irradiation source in this spectroscope. A Michelson interferometer was used to quantify the signal. Spectra comprised 32 scans, with a resolution of 2 cm^{-1}. The sample size was 50 mg.

2.3 Methacrylated vegetable oil synthesis

Epoxidized vegetable oil (500 g with OOC 6.2%, 1.9 molar equiv.) was transferred into a 1000 mL round-bottom flask

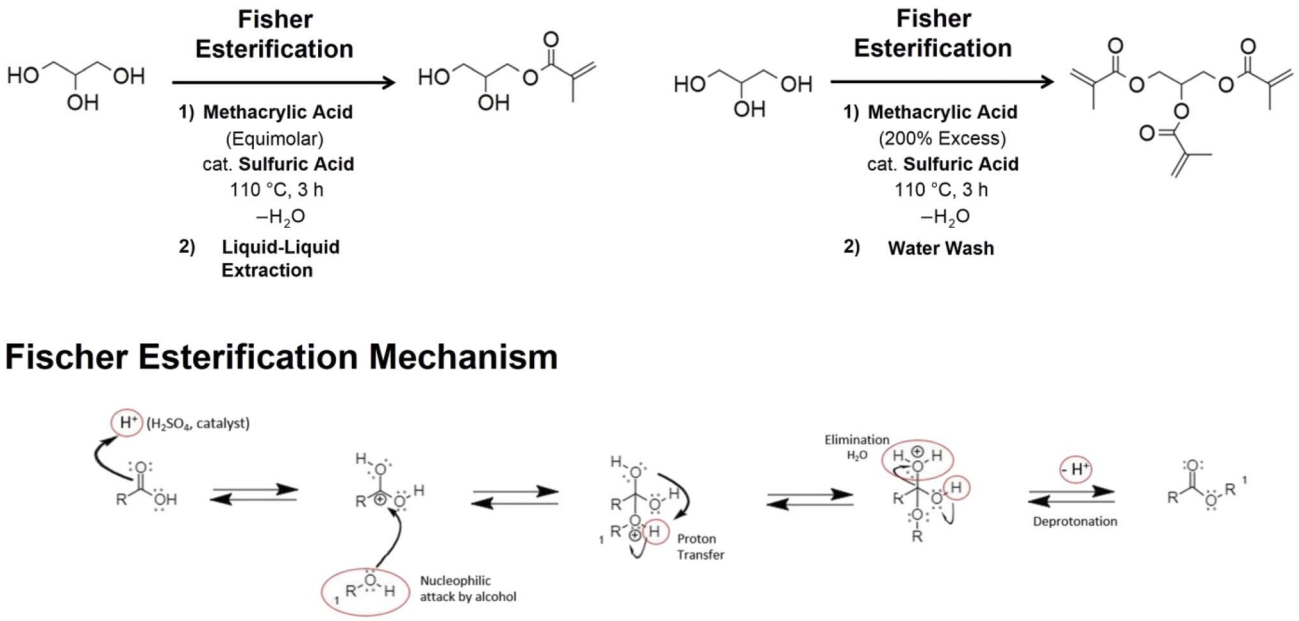

Fig. 3 The reaction scheme of methacrylated glycerol derivative synthesis (glycerol monomethacrylate (MGLY) and glycerol trimethacrylate (TGLY)) through Fischer esterification catalyzed by sulfuric acid. Recreated with permission under a Creative Commons license (http://creativecommons.org/licenses/by/4.0/) from ref. 59 Copyright (2018), MDPI.

together with methacrylic acid (195 g, 1.9 mol). The reaction solution was heated in an oil bath to the reaction temperature (120 °C). After pre-heating, the catalyst (triethylamine, 6 g, 0.06 mol) was added to the reaction batch. The methacrylation reaction (see Fig. 2) was performed until the acid value reached 10 mg KOH per g (representing 91.1% conversion). The purification process involved diluting the product with ethyl acetate (1 : 1 by volume) to reduce viscosity. The diluted crude product was neutralized with a potassium hydroxide solution and washed twice with distilled water to remove the formed salts and the catalyst. Lastly, the diluting ethyl acetate was removed *via* distillation. The pure methacrylated vegetable oil was characterized by ^{1}H NMR and FT-IR analyses.

^{1}H NMR of methacrylated vegetable oil (Fig. S1) (500 MHz, $CDCl_3$): δ 6.12 (d, $J = 1.5$ Hz, 2H), 5.59 (q, $J = 2.1$ Hz, 2H), 4.28 (dd, $J = 11.9$, 4.3 Hz, 2H), 4.17–4.07 (m, 3H), 2.31 (tt, $J = 7.6$, 2.4 Hz, 6H), 2.17–1.88 (m, 12H), 1.75–1.11 (m, 78H), 0.90 (tt, $J = 7.1$, 1.6 Hz, 9H).

The FTIR spectrum of methacrylated vegetable oil (Fig. S2) with wavenumber intervals: O–H stretching at 3550–3200 cm^{-1}, C–H stretching at 3000–2840 cm^{-1}, C=O (ester) stretching at 1750–1735 cm^{-1}, C=C stretching at 1662–1626 cm^{-1}, C–O (ester) stretching at 1210–1163 cm^{-1}, and C=C bending at 840–790 cm^{-1}.

2.4 Methacrylated glycerol derivative synthesis

Two different derivatives were synthesized – the mono-functional glycerol monomethacrylate (MGLY) and the multi-functional glycerol trimethacrylate (TGLY) (see Table 1). The MGLY synthesis involved three reactants: glycerol (92 g, 1 mol), methacrylic acid (86 g, 1 mol), and sulfuric acid (0.98 g, 0.01 mol). Glycerol and the catalyst were mixed in a three-necked 500 mL round-bottom flask in an oil bath at 110 °C. Methacrylic acid was continuously added to the reaction mixture using a dripping funnel for 30 minutes. Equimolar esterification (see Fig. 3) was performed for 3 hours until the reaction mixture reached an acid value of 26 mg KOH per g (representing 91.7% conversion). The reaction water was removed by vacuum distillation at 200 torr. The purification involved mixing the crude product in ethyl acetate (1 : 1 by volume). Then we neutralized the remaining methacrylic and sulfuric acid and quenched the mixture with water. Finally, the neutralized and purified product was separated from ethyl acetate by distillation.

The MGLY synthesis also involved three reactants: glycerol (92 g, 1 mol), methacrylic acid (258 g, 3 mol), and sulfuric acid (0.98 g, 0.01 mol). The reaction mixture contained glycerol and methacrylic acid and was pre-heated to 110 °C. After the pre-heating, the catalyst was introduced. The molar excess esterification lasted 3 hours, during which the acid value reached 30 mg KOH per g (representing 93.8% conversion). The reaction water was removed by vacuum distillation at 200 torr. After the reaction, the synthesized TGLY was neutralized with potassium hydroxide (water solution) and washed with distilled water. The purified TGLY was dried over anhydrous sodium sulfate. The synthesized MGLY and TGLY were characterized by ^{1}H NMR, ESI-MS, and FT-IR.

^{1}H NMR of glycerol monomethacrylate (MGLY) (Fig. S3) (500 MHz, $CDCl_3$): δ 6.15 (q, $J = 1.2$ Hz, 1H), 5.65–5.57 (m, 1H), 4.36–4.15 (m, 2H), 4.15–3.75 (m, 1H), 3.72–3.44 (m, 2H), 1.96 (t, $J = 1.3$ Hz, 3H).

The FTIR spectrum of glycerol monomethacrylate (MGLY) (Fig. S4) with wavenumber intervals: C–H stretch at 3000–2840 cm^{-1}, C=O (ester) stretch at 1750–1735 cm^{-1}, C=C stretch at 1662–1626 cm^{-1}, C–O (ester) stretch at 1210–1163 cm^{-1}, and C=C bend at 840–790 cm^{-1}.

The ESI-MS (Fig. S5) fragmentation spectrum of glycerol monomethacrylate (MGLY) ($C_7H_{12}O_4$) spectrum calc. $[M - H_2O + H]^+$ 143.2 *m*/*z*, found 142.9 *m*/*z*.

^{1}H NMR of glycerol trimethacrylate (TGLY) (Fig. S6) (500 MHz, $CDCl_3$) δ 6.17–6.05 (m, 3H), 5.61 (dtd, $J = 10.0$, 3.2, 1.6 Hz, 3H), 5.44 (tt, $J = 6.0$, 4.4 Hz, 1H), 4.46–4.15 (m, 4H), 1.95 (dt, $J = 12.7$, 1.4 Hz, 9H).

The FTIR spectrum of glycerol trimethacrylate (TGLY) (Fig. S7) with absorption wavenumber intervals: C–H stretch at 3000–2840 cm^{-1}, C=O (ester) stretch at 1750–1735 cm^{-1}, C=C stretch at 1662–1626 cm^{-1}, C–O (ester) stretch at 1210–1163 cm^{-1}, and C=C bend at 840–790 cm^{-1}.

The ESI-MS (Fig. S8) fragmentation spectrum of glycerol trimethacrylate (TGLY) ($C_{15}H_{20}O_6$) spectrum calc. $[M - H_2O + H]^+$ 296.3 *m*/*z*, found 296.1 *m*/*z*.

2.5 Rheological study

The synthesized glycerol derivatives were designed to become alternatives to currently used fossil-based reactive diluents. The rheological study was conducted to confirm their diluting character. We used the TA Instruments rheometer AR-G2 (ARES-G2, New Castle, DE, USA) for the investigation. The prepared systems (containing 25 wt% of a particular reactive diluent) were measured under the following conditions: 500 μL of sample, a Peltier platform and cone-plate geometry (40 mm, 2° angle), a shear rate of 10 s^{-1}, and a temperature ramp from 25 to 60 °C. The Arrhenian plot (1) is formulated as follows (1):[30]

$$\ln \eta = \frac{E_a}{R} \cdot \frac{1}{T} + \ln \eta_\infty \quad (1)$$

where the dependence of apparent viscosity ln(η) (−) on the reverse value of temperature $1/T$ (K^{-1}) is constructed. The flow activation energy E_a (J mol^{-1}) is extracted from the slope by multiplying it by the universal gas constant R (J (mol^{-1} K^{-1})). Also, we can obtain the pre-exponential factor (infinite viscosity) η_∞ (Pa s) from the *y*-intercept.

2.6 3D printing of synthesized systems

We used a PRUSA SL1 3D printer (Prusa Research Ltd, Czech Republic) for the experiments. We formulated mixtures containing 25 wt% of each reactive diluent in methacrylated vegetable oil. The prepared systems were mixed with a type I photoinitiator BAPO (1 wt%). The print settings were as follows: the first layer's exposure time was 30 seconds, and all subsequent layers' exposure time was 15 seconds. The set layer thickness was 50 μm. After printing, the samples were cleaned with isopropanol and post-cured under 405 nm LED light for 2 hours.

2.7 The 3D printed specimens' characterization

Dynamic mechanical analysis (DMA) provided information on the glass transition temperature and crosslinking density of the prepared 3D-printed cured systems. We used DMA RSA-G2 from TA Instruments (New Castle, DE, USA). Testing specimens with typical dimensions of 50 × 10 × 4 mm fabricated by additive manufacturing were measured. The specimens were mounted in a dual cantilever geometry and subjected to cyclic deformation with a 25 μm amplitude and a 1 Hz frequency. The samples were heated from room temperature to 120 °C at a rate of 3 °C min^{-1}. The glass-transition temperature (T_g) and the crosslinking density (ν_e) were calculated for all tested systems to provide information regarding the thermoset molecular structure. The equation leading to the ν_e calculation is formulated as follows:[31]

$$\nu_e = \frac{E'}{3RT'} \quad (2)$$

where ν_e is the crosslinking density (mol m^{-3}); E' stands for the storage modulus in the rubbery plateau region (E' at T_g + 40 °C) (Pa); R is the universal gas constant (J (mol^{-1} K^{-1})); and T' is the thermodynamic temperature in the rubbery plateau region (at T_g + 40 °C) (K).

Thermo-gravimetric analysis (TGA) was used to investigate the thermal stability of the synthesized systems. The analysis was conducted on a TGA Q500 from TA Instruments (New Castle, DE, USA). The degradation of a sample (10–15 mg) was monitored using the following heating program: equilibration at 40 °C; heating to 600 °C at 10 °C min^{-1} under N_2; and 10 min at 600 °C under an air atmosphere. The heat-resistant index was obtained from the proposed eqn (3):[32]

$$T_s = 0.49[T_5 + 0.6(T_{30} - T_5)] \quad (3)$$

where T_s is the heat-resistant index (°C); T_5 stands for the temperature at 5% mass loss (°C); and T_{30} stands for the temperature at 30% mass loss (°C).

The mechanical properties of prepared mixtures were determined using tensile and flexural testing. Both tests were performed on a Zwick Z 010 testing machine (ZwickRoell GmbH & Co., Ulm, Germany) equipped with a 500 N load cell. The tensile test was performed according to the CSN EN ISO 527 standard using standardized double-paddle specimens (dogbones 5A) with a 4 × 2 mm cross-sectional area (five specimens were measured). The test speed was set to 5 mm min^{-1}. The flexural test followed CSN EN ISO 178 using standard rectangular specimens with dimensions of 80 × 10 × 4 mm. The loading nose and support radius were 5 mm, with a support span of 64 mm (five specimens were measured). The test speed was set to 10 mm min^{-1}.

2.8 Statistical analysis

Statistical analysis software SPSS-20.0 (IBM product of Chicago, United States) was utilized to analyze the data. The results were presented in terms of arithmetic modules and strengths with standard deviation. The one-way ANOVA test was utilized to provide statistical information regarding the performed tensile and flexural tests. *Post hoc* Tukey's test was performed to

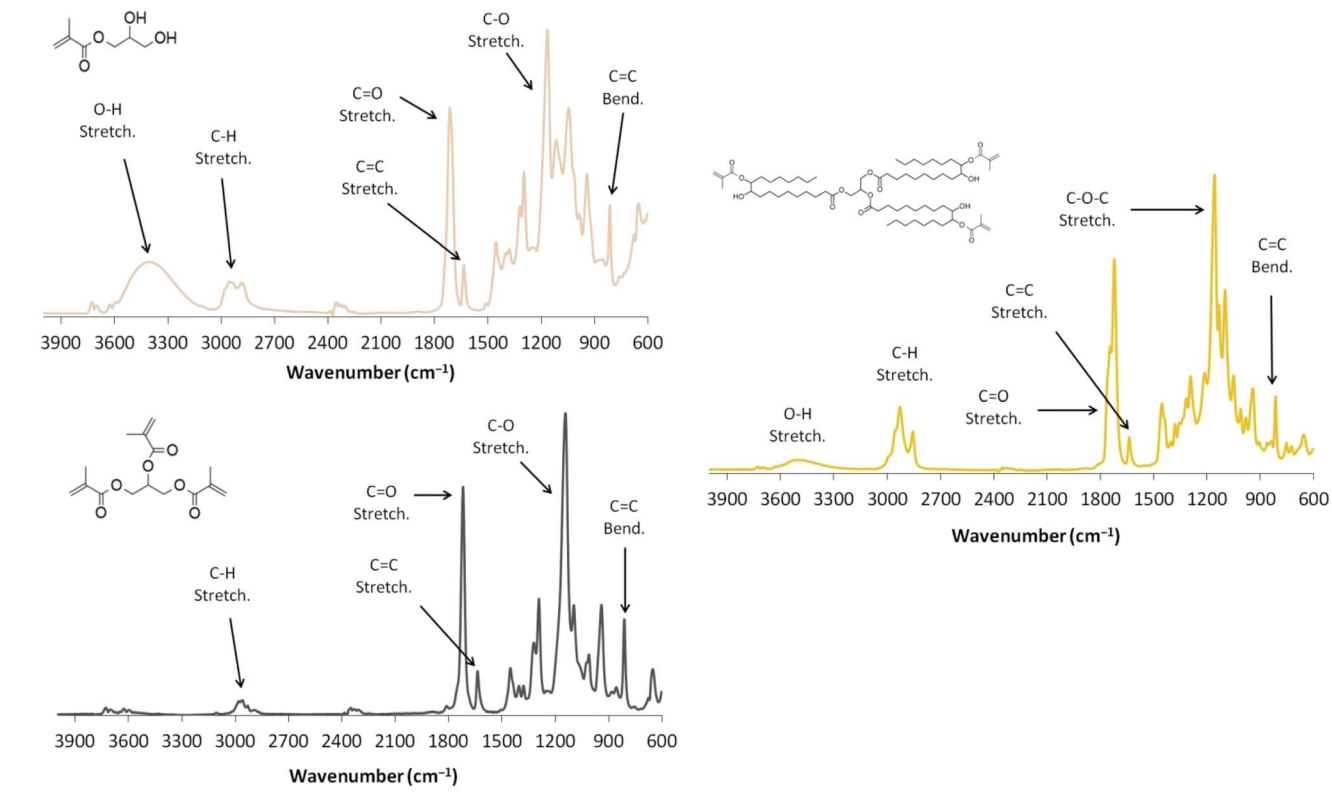

Fig. 4 The FTIR spectra of the synthesized products MO, MGLY, and TGLY.

compare the difference of values among the tested polymerized systems. The significance level was located when p-value ≤ 0.05.

3 Results and discussion

3.1 Synthesized systems' structural analysis

The bio-based curable precursors, methacrylated vegetable oil and methacrylated glycerol derivatives, were synthesized *via* a nucleophilic substitution and the Fischer esterification using methacrylic acid as a functionalizing agent. This approach is typical for curable triacylglycerides;[15,33] however, modified glycerol is usually synthesized using more reactive carboxylic derivatives. Typically, acyl halides,[34] anhydrides,[35] or esters[36] are used for the synthesis of curable modified glycerol derivatives, which increases the process's cost and complicates the up-scaling and manipulation due to the increased toxicity. Also, these approaches are environmentally unfriendly due to their toxicity, potential VOC generation, and the disposal of secondary products (such as hydrochloric acid or the secondary carboxylic acid formed). The Fischer esterification approach, coupled with vacuum distillation of the forming water, addresses many of the listed issues. Methacrylic acid is much less volatile than other reactive derivatives, reducing associated risks and VOC emissions. Additionally, the secondary reaction product is efficiently disposable water, rather than the halide acid, carboxylic acid, or volatile alcohol from transesterification. The structural characterization of the obtained bio-based curable products was carried out using a range of instrumental methods.

We present the ^{1}H NMR results in Fig. 5 together with the visual appearance of the synthesized compounds. All products were also characterized and confirmed by FT-IR (see Fig. 4), and the glycerol derivatives were confirmed using ESI-MS analysis (see the results in Fig. S5 and S8). The chemical structures of the synthesized products (MO, MGLY, and TGLY) and the reference compounds (EGDA and HEMA) are summarized in Table 2, along with the bio-based content values. The bio-based content represents the overall weight of materials obtained from renewable sources, which is significant for suggesting suitable substitutes for fossil-based systems. Moreover, our proposed synthesis path offers a much safer and more efficient production approach than EGDA and HEMA synthesis. The reference fossil-based diluents are fabricated from toxic and volatile compounds (ethylene oxide and acryloyl halide), which not only exclude bio-based content from the final product but also require specialized production steps to yield the final molecules.[54,55] Our esterification approach involves only the condensation reaction, in which water is formed as a byproduct. Therefore, the direct esterification promises a significantly more efficient and rational production route.

The obtained ^{1}H NMR spectra confirm all protons present in the synthesized bio-based structures. The typical alkene signals occur in the same chemical shift interval for all the synthesized molecules (6.25–5.50 ppm). This functional group is the most essential part of the structures since it is responsible for curability properties. The inner carbon backbone protons in the chemical shift range of 4.50–3.50 ppm are crucial for characterizing the present glycerol and its derivatives. The methacrylated vegetable oil (Fig. 5, top) and glycerol trimethacrylate (Fig. 5, bottom) exhibit the same proton signals in this chemical shift interval. This confirms the complete methacrylation of TGLY, as this result is identical to that of other fully esterified

Table 2 The chemical structures and bio-based contents summarized for the studied molecules

Molecule	Structure	Bio-based content
MO	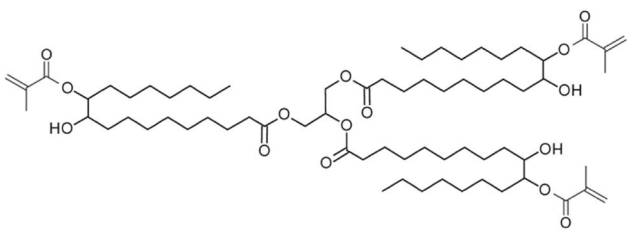	77.1 wt%
MGLY	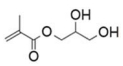	57.5 wt%
TGLY	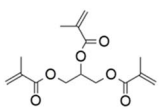	31.1 wt%
EGDA	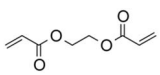	0 wt%
HEMA	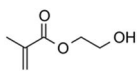	0 wt%

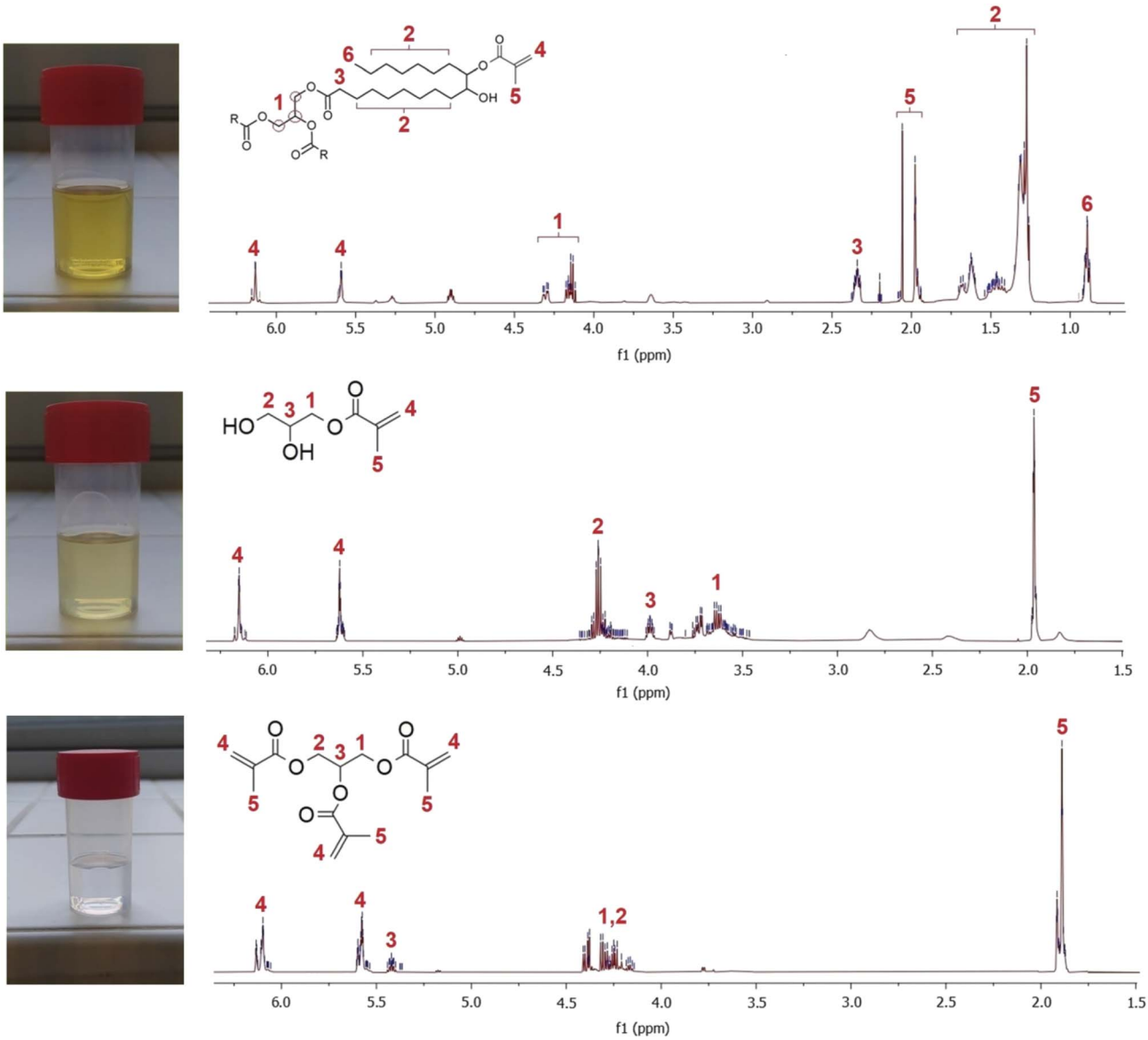

Fig. 5 The ^{1}H NMR spectra and the appearance images of the synthesized products – methacrylated vegetable oil (top), glycerol monomethacrylate (middle), and glycerol trimethacrylate (bottom).

glycerol derivatives.[37] In contrast, the MGLY's ^{1}H NMR spectrum (Fig. 5, middle) uncovers the signal shifts due to the free hydroxyl appearance (confirmed by FT-IR and ESI-MS). In addition to the calculation of integrated protons (see SI, Fig. S1, S3, and S6), the chemical structures of all synthesized products were verified. FT-IR and ESI-MS analyses were used not only to confirm the chemical structure but also to identify free hydroxyl groups. Since the d-chloroform used is not ideal for the study of hydroxyl groups,[38] the presence of hydroxyl groups in the produced compounds was confirmed using these methods.

3.2 The diluting properties of the synthesized glycerol derivatives

The modified triacylglycerides used as photo-curable resins typically exhibit high viscosity.[10] The primary purpose of the synthesized TGLY and MGLY is to decrease the viscosity while incorporating into the formed thermoset molecular structure. Usually, non-polar, entirely functionalized curable compounds, such as EGDA, have very low viscosity due to their low molecular weight and the absence of polar or hydrogen-bonding functional groups.[13] Although HEMA contains one free hydroxyl functional group, its viscosity remains very low due to the molecular weight of its structure.[39] We performed the rheological study, uncovering the diluting effect of the synthesized TGLY and MGLY compared to the commercially used EGDA and HEMA. The synthesized compounds represent structural alternatives to the fossil-based molecules. TGLY contains only ester functional groups, without any polar, hydrogen-bond-forming free hydroxyl groups (similar to EGDA). At the same time, MGLY serves as an alternative to HEMA, containing two free hydroxyl groups and possessing a high bio-based content (57.5 wt%). The results describing the rheological character of

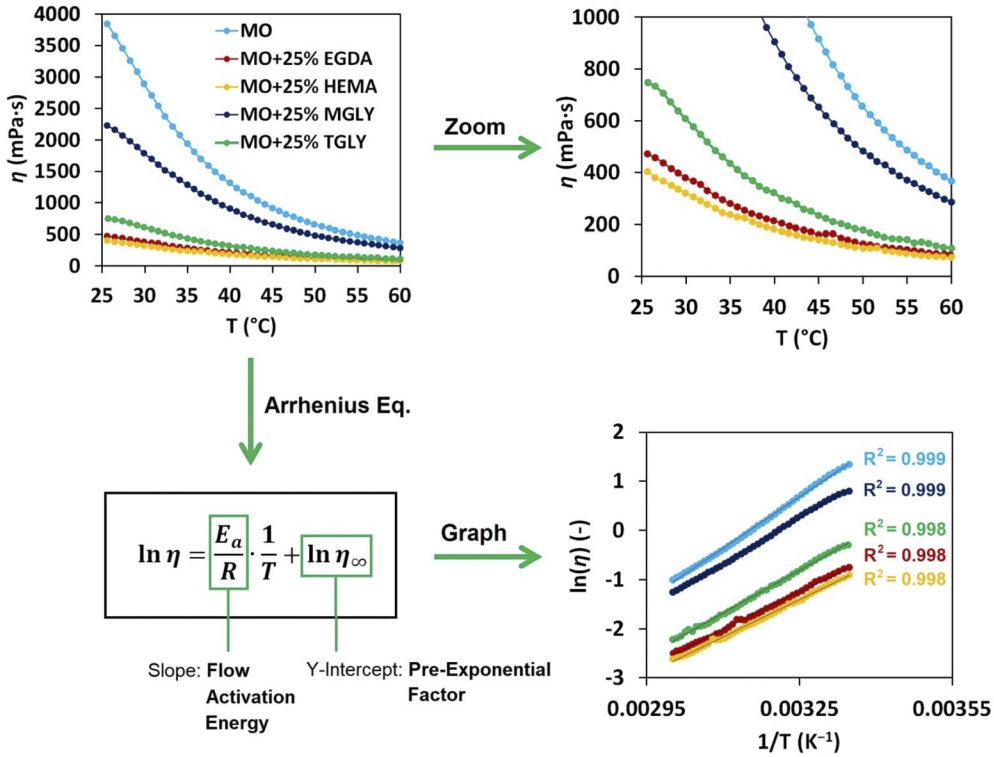

Fig. 6 The rheological investigation of diluted methacrylate vegetable oil (MO) systems containing 25 wt% of the reactive diluent used (top left) and a zoom-in (top right). The graphical interpretation of the Arrhenius equation (bottom left) applied to the investigated systems (bottom right).

the systems containing 25 wt% of the reactive diluent (a typical weight content used for additive manufacturing)[40] are summarized and graphically interpreted in Fig. 6. The numerical values calculated from the Arrhenius equation are listed in Table 3.

The rheological investigation uncovered several advantages of the commercial reactive diluents over the bio-based synthesized compounds. The most critical parameters, the apparent viscosity at 30 °C ($\eta_{30°C}$) and the flow activation energy (E_a), reached lower values for the measured oil-diluent systems containing HEMA ($\eta_{30°C}$ reaching 314 mPa s and E_a reaching 42.0 kJ mol^{-1}) and EGDA ($\eta_{30°C}$ reaching 372 mPa s and E_a reaching 43.1 kJ mol^{-1}). The produced glycerol-based derivatives exhibited diluting properties, but MGLY primarily decreased the system's viscosity the most ($\eta_{30°C}$ reaching 1745 mPa s and E_a reaching 51.4 kJ mol^{-1}). This outcome is mainly due to the two vacant hydroxyl groups, which can form numerous hydrogen-bonding interactions and increase the polarity of the reactive diluent.[41] On the other hand, TGLY reached higher viscosity and activation energy levels compared to the commercial diluents ($\eta_{30°C}$ reaching 590 mPa s and E_a reaching 48.4 kJ mol^{-1}), but these values are competitive with those of the fossil-based systems. The absence of hydrogen-bond-forming functional groups contributes significantly to TGLY's diluting character, even given its highest molecular weight among the studied systems. Not only do the molecules of MGLY form hydrogen bonding with each other, but also with the MO diluted system through the free hydroxyls generated after the nucleophilic substitution (see Fig. 2). Considering all aspects of the synthesized reactive diluents compared to commercial alternatives, TGLY has greater substituting potential than MGLY. The least-diluting character of the MGLY-containing MO system is comparable to that of published systems involving epoxidized cardanol monomers (ECA), which possess higher viscosity.[50] The rest of the diluents (EGDA, HEMA, and TGLY) reached similar viscosity values to the unsaturated esters (UES) derived from furan monomers.[51]

Table 3 The results of the rheological investigation

Rheology				
System	$\eta_{30°C}$ (mPa s)	η_∞ (mPa s)	E_a (kJ mol^{-1})	R^2
MO	2791	2.67×10^{-7}	58.2	0.999
MO + 25% EGDA	372	1.40×10^{-5}	43.1	0.998
MO + 25% HEMA	314	1.79×10^{-5}	42.0	0.998
MO + 25% MGLY	1745	2.44×10^{-6}	51.4	0.999
MO + 25% TGLY	590	2.74×10^{-6}	48.4	0.998

3.3 Thermal and thermo-mechanical investigation

The 3D-printed specimens were investigated for thermal stability and thermo-mechanical properties to provide a comprehensive review of the characteristics of the processed precursor systems. The thermal stability, represented by the heat-resistant index (T_s), includes information on the chemical stability of the molecular site structure formed. It also describes

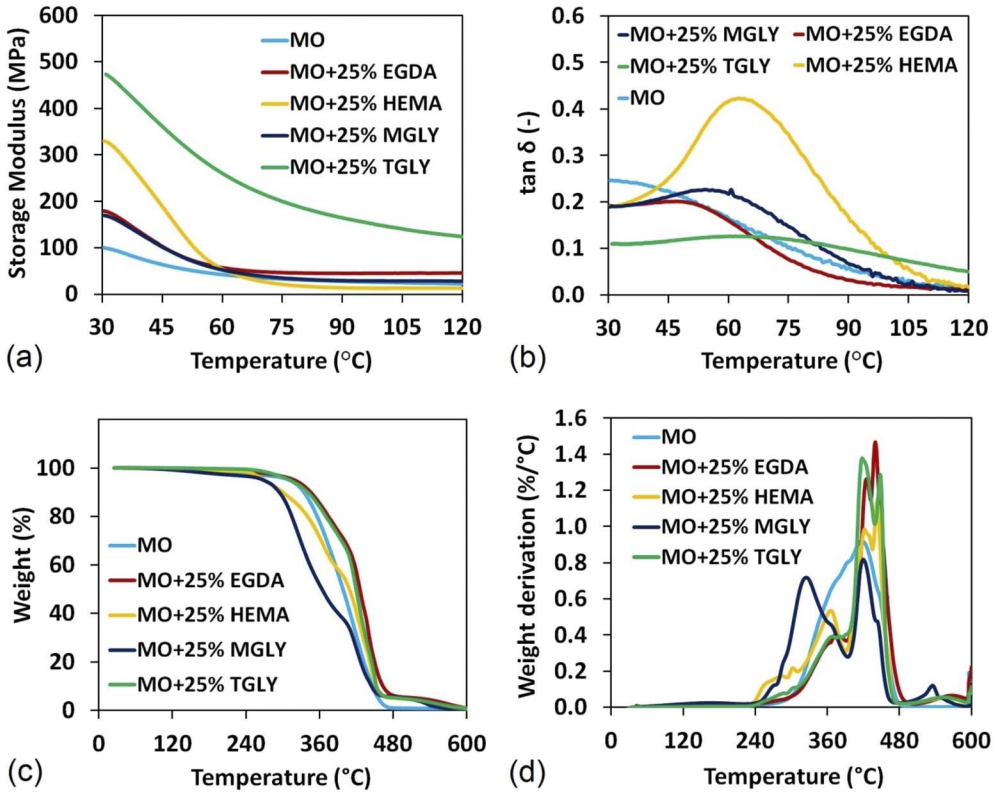

Fig. 7 (a)The measured storage modules from DMA, (b) the calculated tan δ values from DMA, (c) the thermal degradation provided by TGA, and (d) the derivative of the degradation curve.

the most unstable chemical bonding in the thermoset, giving an idea of the potential manufacturing focus. The thermo-mechanical characterization contributes to the general mechanical description of the produced materials. The measured glass-transition temperature (T_g) and the calculated crosslinking density (ν_e) provide an overview of the potential positive and adverse outcomes in the particular applications. Also, since we investigated MO-based systems containing mono-functional reactive diluents (HEMA and MGLY) and multi-functional reactive diluents (EGDA and TGLY), their effects on the overall thermal stability and the rigidity of the cured thermoset are significant for comparison purposes. The graphical results of the DMA analysis are shown in Fig. 7a and b, while the TGA results are shown in Fig. 7c and d. The measured parameters from TGA used for the calculation of T_s, together with the DMA-measured values, T_g, and the calculated ν_e, are summarized in Table 4.

The DMA results uncovered that MO containing TGLY as a reactive diluent reached the highest storage modulus at 30 °C ($E' = 473$ MPa) and the crosslinking density ($\nu_e = 15.5$ kmol m^{-3}). The reached T_g of the TGLY system was the second-highest ($T_g = 61.7$ °C), followed by the MO system with HEMA ($T_g = 62.5$ °C). The highest rigidity of the TGLY-containing system is caused by the multi-functional character of this compound, containing three polymerizable functional groups. This exceptional rigidity was observed in other curable systems containing multi-functional reactive diluents.[42] The system containing HEMA reached the second highest storage modulus

Table 4 The results and calculated parameters from TGA and DMA analyses

Thermal/thermo-mechanical properties							
TGA				DMA			
System	T_5 (°C)	T_{30} (°C)	T_s (°C)	$E'_{30°C}$ (MPa)	$E''_{30°C}$ (MPa)	T_g (°C)	ν_e (kmol m^{-3})
MO	310.6	371.8	170.2	100	25	<30.0*	4.6
MO + 25% EGDA	318.8	400.7	180.3	179	34	47.1	5.0
MO + 25% HEMA	270.7	362.8	159.7	330	63	62.5	1.4
MO + 25% MGLY	268.4	329.1	149.4	169	32	60.7	3.1
MO + 25% TGLY	311.2	395.7	177.3	473	52	61.7	15.5

Table 5 The statistical deviations obtained from the tensile and flexural measurements

Mechanical test deviations				
System	Tensile modulus	Tensile strength	Flexural modulus	Flexural strength
MO	1.5%	12.4%	6.9%	8.2%
MO + 25% EGDA	5.3%	6.0%	3.1%	3.1%
MO + 25% HEMA	5.9%	7.7%	6.1%	7.6%
MO + 25% MGLY	3.5%	15.5%	7.7%	6.4%
MO + 25% TGLY	3.0%	6.1%	6.4%	27.0%

at 30 °C ($E' = 330$ MPa), and together with a high T_g value, the HEMA-containing thermoset exhibits the second-best thermo-mechanical character. According to the literature, this result may be affected by the attractive interaction between the free hydroxyl group of HEMA and the MO molecular structure.[43] Regarding the crosslinking density, the HEMA-containing thermoset reached the lowest value ($\nu_e = 1.4$ kmol m^{-3}), which corresponds with its functionality. Strangely, EGDA exhibited the second-lowest storage modulus at 30 °C ($E' = 179$ MPa) and the lowest glass-transition temperature ($T_g = 47.1$ °C), despite having a two-functional structure. The MGLY-containing system exhibited higher T_g (60.7 °C) and almost similar $E'_{30°C}$ (169 MPa) to the EGDA system, which may confirm the significant impact of the polar hydrogen-bonding-forming groups on the eventual thermo-mechanical performance. The similar DMA glass-transition temperatures were measured for the oligomer PLA-derived methacrylates used for SLA 3D printing (particularly the longest oligomers). However, the reported systems that achieved similar thermomechanical properties could not be printed. Our presented and suggested system was processed without any issues.[11] Despite all the used systems improving the thermo-mechanical performance of the pure MO system, TGLY and HEMA resulted as the best performing systems, promising improved mechanical performance.

The TGA analysis revealed that two systems, MO with EGDA/TGLY, increased the heat-resistant index of the cured 3D printed thermoset. This outcome corresponds with the crosslinking density calculated from DMA. The MO + 25% EGDA system reached the highest T_s value (180.3 °C), followed by the MO + 25% TGLY system ($T_s = 177.3$ °C). Based on the previously obtained results, the higher crosslinked thermosets exhibited better heat resistance due to more durable molecular sites.[44] The differences between glycerol and ethylene glycol esters might influence the heat-resistance results since TGLY in MO provided higher crosslinking density but resulted in lower resistance. The structural stability of acrylate esters was confirmed in the published literature.[45] The MO systems with MGLY and HEMA reached lower thermal resistances (MGLY heat-resistant index $T_s = 149.4$ °C and HEMA's value of 159.7 °C) than the pure MO thermoset ($T_s = 170.2$ °C). This outcome verifies the decreasing thermal stability of the less crosslinked

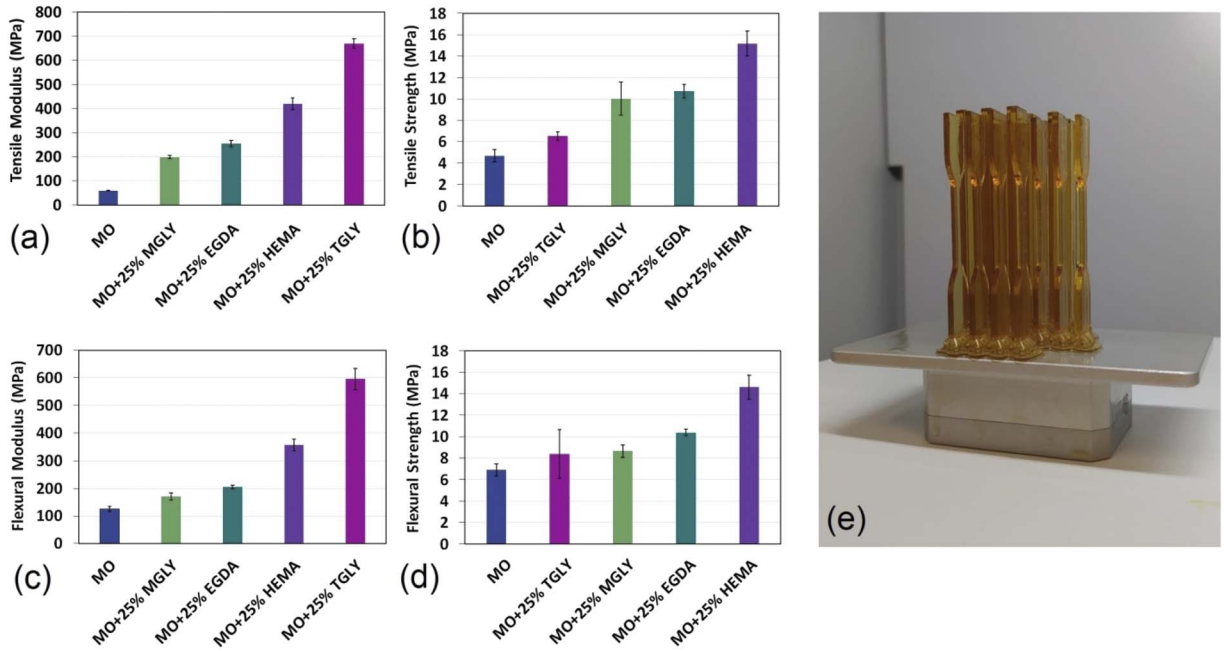

Fig. 8 The results of the mechanical tests. (a) Tensile moduli, (b) tensile strengths, (c) flexural moduli, (d) flexural strengths, and (e) the image of the 3D printed testing specimens.

resins. The applied 3D printing technology is widely used in low-temperature applications; therefore, the measured thermal resistances of all investigated systems were similar to those of the published and used systems.[46]

3.4 Mechanical performance

To determine the mechanical properties of 3D printed samples, tensile and flexural tests were conducted. The statistical data (calculated deviations) are summarized in Table 5 (and shown as error bars in Fig. 8). From the results of the tensile test (see Fig. 8), it can be observed that all samples containing a reactive diluent showed an increase in both the elastic modulus and tensile strength compared to methacrylated rapeseed oil (MO; measured value 58 ± 1 MPa) alone. The highest elastic modulus was observed in the TGLY-containing sample (669 ± 20 MPa). This is likely due to the diluent's structure, which contains three double bonds capable of crosslinking. As the crosslinking density increases, the modulus increases.[47] In contrast, the MO + 25% MGLY sample (198 ± 7 MPa), which contains only one double bond, exhibited the lowest modulus after MO, likely due to lower crosslinking density. Interestingly, the MO + 25% HEMA sample (420 ± 25 MPa), which also contains only one double bond, showed a slightly higher modulus than samples containing MGLY. This could be attributed to the fact that the HEMA used forms molecular interactions with MO through H-bonding. The system containing MGLY also contains free hydroxyls (two in total), but their chemical structure may cause an adverse effect on the mechanical performance (based on previous findings).[48]

Regarding tensile strength, the MO + 25% HEMA samples (15.2 ± 1.2 MPa) demonstrated the highest values, whereas the MO + 25% TGLY samples (6.5 ± 0.4 MPa) exhibited the lowest, reflecting brittle behavior (also evident in their stress–strain curves). This behavior is likely due to the formation of a denser, crosslinked network in samples with TGLY. Interestingly, the MO + 25% MGLY (10.0 ± 1.6 MPa) and MO + 25% EGDA samples (10.7 ± 0.6 MPa) showed comparable mechanical performance, despite differences in their molecular structures.

In the case of the flexural test (see Fig. 8), the exact behavior of the samples was observed – the highest flexural modulus was achieved by the samples containing TGLY (596 ± 38 MPa), whereas the lowest modulus among samples containing

Table 6 The one-way ANOVA results[a]

Mechanics				
System	Tensile modulus (MPa)	Tensile strength (MPa)	Flexural modulus (MPa)	Flexural strength (MPa)
MO	58.3 ± 0.8	4.67 ± 0.58	125.9 ± 8.7	6.91 ± 0.57
MO + 25% EGDA	253.4 ± 13.4	10.73 ± 0.64	205.1 ± 6.3	10.36 ± 0.32
MO + 25% HEMA	419.9 ± 24.8	15.17 ± 1.18	356.1 ± 21.8	14.61 ± 1.12
MO + 25% MGLY	197.6 ± 7.0	10.03 ± 1.56	170.4 ± 13.1	8.64 ± 0.55

System	Diluent content		Difference	*F*-ratio	*p*-Value
Tensile modulus					
EGDA-diluted	0%	25%	195.1	1975.788	<0.001*
HEMA-diluted	0%	25%	361.6	1062.536	<0.001*
MGLY-diluted	0%	25%	139.3	1715.352	<0.001*
TGLY-diluted	0%	25%	610.7	4070.704	<0.001*
Tensile strength					
EGDA-diluted	0%	25%	6.06	221.847	<0.001*
HEMA-diluted	0%	25%	10.50	321.026	<0.001*
MGLY-diluted	0%	25%	5.36	74.184	<0.001*
TGLY-diluted	0%	25%	1.85	40.368	<0.001*
Flexural modulus					
EGDA-diluted	0%	25%	79.2	281.159	<0.001*
HEMA-diluted	0%	25%	230.2	485.670	<0.001*
MGLY-diluted	0%	25%	44.5	40 656	<0.001*
TGLY-diluted	0%	25%	470.2	715.951	<0.001*
Flexural strength					
EGDA-diluted	0%	25%	3.45	141.965	<0.001*
HEMA-diluted	0%	25%	7.70	189.118	<0.001*
MGLY-diluted	0%	25%	1.73	23.901	0.001*
TGLY-diluted	0%	25%	1.47	1.989	0.196*

[a] Statistically significant at $p \leq 0.05$.

Table 7 The Tukey's *post hoc* test[a]

Tukey's *post hoc* test		
System	Tensile modulus (MPa)	Statistically significant difference (SSD)
MO	58.3 ± 0.8	MO + 25% EGDA, MO + 25% HEMA, MO + 25% MGLY, MO + 25% TGLY
MO + 25% EGDA	253.4 ± 13.4	MO, MO + 25% HEMA, MO + 25% MGLY, MO + 25% TGLY
MO + 25% HEMA	419.9 ± 24.8	MO, MO + 25% EGDA, MO + 25% MGLY, MO + 25% TGLY
MO + 25% MGLY	197.6 ± 7.0	MO, MO + 25% EGDA, MO + 25% HEMA, MO + 25% TGLY
MO + 25% TGLY	669.0 ± 19.8	MO, MO + 25% EGDA, MO + 25% HEMA, MO + 25% MGLY
Tukey's *post hoc* test		
System	Tensile strength (MPa)	Statistically significant difference (SSD)
MO	4.67 ± 0.58	MO + 25% EGDA, MO + 25% HEMA, MO + 25% MGLY, MO + 25% TGLY
MO + 25% EGDA	10.73 ± 0.64	MO, MO + 25% HEMA, MO + 25% MGLY, MO + 25% TGLY
MO + 25% HEMA	15.17 ± 1.18	MO, MO + 25% EGDA, MO + 25% MGLY, MO + 25% TGLY
MO + 25% MGLY	10.03 ± 1.56	MO, MO + 25% EGDA, MO + 25% HEMA, MO + 25% TGLY
MO + 25% TGLY	6.52 ± 0.40	MO, MO + 25% EGDA, MO + 25% HEMA, MO + 25% MGLY
Tukey's *post hoc* test		
System	Flexural modulus (MPa)	Statistically significant difference (SSD)
MO	125.9 ± 8.7	MO + 25% EGDA, MO + 25% HEMA, MO + 25% MGLY, MO + 25% TGLY
MO + 25% EGDA	205.1 ± 6.3	MO, MO + 25% HEMA, MO + 25% MGLY, MO + 25% TGLY
MO + 25% HEMA	356.1 ± 21.8	MO, MO + 25% EGDA, MO + 25% MGLY, MO + 25% TGLY
MO + 25% MGLY	170.4 ± 13.1	MO, MO + 25% EGDA, MO + 25% HEMA, MO + 25% TGLY
MO + 25% TGLY	596.1 ± 38.4	MO, MO + 25% EGDA, MO + 25% HEMA, MO + 25% MGLY
Tukey's *post hoc* test		
System	Flexural strength (MPa)	Statistically significant difference (SSD)
MO	6.91 ± 0.57	MO + 25% EGDA, MO + 25% HEMA, MO + 25% MGLY, MO + 25% TGLY
MO + 25% EGDA	10.36 ± 0.32	MO, MO + 25% HEMA, MO + 25% MGLY, MO + 25% TGLY
MO + 25% HEMA	14.61 ± 1.12	MO, MO + 25% EGDA, MO + 25% MGLY, MO + 25% TGLY
MO + 25% MGLY	8.64 ± 0.55	MO, MO + 25% EGDA, MO + 25% HEMA, MO + 25% TGLY
MO + 25% TGLY	*p*-Value > 0.05	*p*-Value > 0.05

[a] SSD from the tested group at a $p \leq 0.05$ level of significance.

diluents was measured in MO + 25% MGLY (170 ± 13 MPa). Regarding flexural strength, a similar increasing trend was observed to the tensile test. The lowest value was measured for the MO sample without diluents (6.9 ± 0.6 MPa), and among the samples with diluents, the lowest strength was observed in those containing TGLY (8.38 ± 2.27 MPa), followed by samples with MGLY (8.6 ± 0.6 MPa) and EGDA (10.4 ± 0.3 MPa), while the highest strength was achieved again by the sample containing commercial diluent – HEMA (14.6 ± 1.1 MPa). The complete statistical results provided using IBM SPSS Statistics (provided the one-way ANOVA followed by Tukey's post hoc test) are summarized in Tables 6 and 7.

Overall, the addition of a reactive diluent had a positive effect on both mechanical tests, increasing the modulus and strength. This demonstrates that diluents play a beneficial role: they improve the material's mechanical performance by enhancing stiffness and strength. The obtained tensile parameters are comparable to those reported in the literature, focusing on the polyurethane-acrylic resin diluted with *N*-acryloyl-morpholine (ACMO).[52] The nominal parameters obtained from the flexural mechanical tests also correspond with a particular investigated curable system derived from epoxidized and acrylated soybean oil.[53] Although two promising bio-based reactive diluents, MGLY and TGLY, were suggested, synthesized, and characterized, their renewable content could still be higher. If acrylic acid were used instead of methacrylic acid, the bio-based content would increase, but overall toxicity and process inefficiency would also increase. Additionally, the proposed MGLY still lacks sufficient diluting character. An appropriate mixture of glycerol derivatives would enhance the diluting properties.

4 Conclusions

This work aims to suggest, synthesize, and characterize bio-based alternatives to the commercially used reactive diluents, 2-hydroxyethyl methacrylate (HEMA) and ethylene glycol diacrylate (EGDA), based on functionalized glycerol. The synthesized glycerol monomethacrylate (MGLY) and glycerol

trimethacrylate (TGLY) were mixed with the synthesized methacrylated vegetable oil (MO) to decrease its excessively viscous profile. The synthesized structures were structurally confirmed by cross-analysis, including ^{1}H NMR, FT-IR, and ESI-MS. We performed a rheological study verifying the functional character. The working systems were prepared with 75 wt% MO and 25 wt% of the particular reactive diluent. The commercial HEMA and EGDA outperformed both glycerol derivatives; however, TGLY reached values that were both sufficient and competitive with those of the fossil-based compounds. DMA analysis revealed that the TGLY-containing thermoset has the most rigid structure, owing to its highest crosslinking density. According to the DMA, the MGLY-containing system outperformed the EGDA-containing system, except for the crosslinking density. The systems containing TGLY and EGDA improved MO's thermal resistance by enhancing the molecular site formed. The mechanical tests showed that the TGLY-based thermoset exhibited the highest tensile and flexural moduli, owing to its greater rigidity and crosslinking density. The HEMA-based systems reached the best tensile and flexural strengths. Both the glycerol derivatives, TGLY and MGLY, fulfilled their reactive diluting purpose. TGLY improved all the studied rheological, thermal, thermo-mechanical, and mechanical properties of the eventual thermoset. The study comprehensively describes the direct alternatives, monofunctional MGLY and multi-functional TGLY, and uncovers their positive and adverse effects on the photo-cured, 3D printed bio-based resin. The results confirm their potential as substitutes for the subsequently investigated commercial diluents, EGDA and HEMA. The sustainable aspect, linked to the overall bio-based content and the considered chemical synthesis, exceeds the currently set standards for producing fossil-based diluents.

Conflicts of interest

There are no conflicts to declare.

Data availability

The data supporting this article have been included as part of the electronic supplementary information (SI). Supplementary information is available. See DOI: https://doi.org/10.1039/d5su00891c.

Acknowledgements

V. J. acknowledges the financial support from the Ministry of Education, Youth and Sports of the Czech Republic (project no. FCH-S-25-8836).

References

1 Q. Yuan, Z. Wang, H. Yao, J. Huang, S. Zuo and H. Huang, Comparative Study Of Reactive Diluents With Different Molecular Structures On The Curing Properties Of Epoxy Adhesives And The Interface Bonding Properties With Mortar, *Int. J. Adhes. Adhes.*, 2023, **126**, 103473, DOI: 10.1016/j.ijadhadh.2023.103473.

2 L. Pastarnokienė, J. Jonikaitė-Švėgždienė, N. Lapinskaitė, R. Kulbokaitė, A. Bočkuvienė, T. Kochanė and R. Makuška, The Effect Of Reactive Diluents On Curing Of Epoxy Resins And Properties Of The Cured Epoxy Coatings, *J. Coat. Technol. Res.*, 2023, **20**(4), 1207–1221, DOI: 10.1007/s11998-022-00737-4.

3 V. Jašek, J. Prokeš, O. Bartoš, J. Fučík, R. Přikryl and S. Figalla, Biobased Nonvolatile Rheology Modifier As A Superior Alternative To Styrene For Pultrusion, *ACS Sustain. Chem. Eng.*, 2025, **13**(27), 10292–10298, DOI: 10.1021/acssuschemeng.5c03049.

4 Y. Catel, J. Angermann, P. Fässler, U. Fischer, T. Schnur and N. Moszner, High Refractive Index Monofunctional Monomers As Promising Diluents For Dental Composites, *Dent. Mater.*, 2021, **37**(2), 351–358, DOI: 10.1016/j.dental.2020.11.029.

5 S. Pérocheau Arnaud, N. M. Malitowski, K. Meza Casamayor and T. Robert, Itaconic Acid-Based Reactive Diluents For Renewable And Acrylate-Free Uv-Curing Additive Manufacturing Materials, *ACS Sustain. Chem. Eng.*, 2021, **9**(50), 17142–17151, DOI: 10.1021/acssuschemeng.1c06713.

6 A. R. Jagtap and A. More, Developments In Reactive Diluents: A Review, *Polym. Bull.*, 2021, **79**(8), 5667–5708, DOI: 10.1007/s00289-021-03808-5.

7 A. D. Tulegenkyzy, P. S. M. Megat-Yusoff, K. M. Al Azzam, B. L. Kairatovna, A. Goyal, G. Eshmaiel, E. Negim, E. Kusrini and M. Samy, Tailoring Epoxy Resin Properties Using Glycidyl Methacrylate-Based Reactive Diluents: Viscosity Reduction And Performance Enhancemen, *Int. J. Technol.*, 2025, **16**(4), 1421, DOI: 10.14716/ijtech.v16i4.7687.

8 L. Papadopoulos, L. Pezzana, N. Malitowski, M. Sangermano, D. N. Bikiaris and T. Robert, Influence Of Reactive Diluent Composition On Properties And Bio-Based Content Of Itaconic Acid-Based Additive Manufacturing Materials, *Discover Appl. Sci.*, 2024, **6**(6), 290, DOI: 10.1007/s42452-024-05926-x.

9 S. Keck, O. Liske, K. Seidler, B. Steyrer, C. Gorsche, S. Knaus and S. Baudis, Synthesis Of A Liquid Lignin-Based Methacrylate Resin And Its Application In 3D Printing Without Any Reactive Diluents, *Biomacromolecules*, 2023, **24**(4), 1751–1762, DOI: 10.1021/acs.biomac.2c01505.

10 C. Vazquez-Martel, L. Becker, W. V. Liebig, P. Elsner and E. Blasco, Vegetable Oils As Sustainable Inks For Additive Manufacturing: A Comparative Study, *ACS Sustain. Chem. Eng.*, 2021, **9**(49), 16840–16848, DOI: 10.1021/acssuschemeng.1c06784.

11 S. Figalla, V. Jašek, J. Fučík, P. Menčík and R. Přikryl, Poly(Lactide) Upcycling Approach Through Transesterification For Stereolithography 3D Printing, *Biomacromolecules*, 2024, **25**(10), 6645–6655, DOI: 10.1021/acs.biomac.4c00840.

12 P. Samyn, J. Bosmans and P. Cosemans, Role Of Bio-Based And Fossil-Based Reactive Diluents In Epoxy Coatings With Amine And Phenalkamine Crosslinker, *Polymers*, 2023, **15**(19), 3856, DOI: 10.3390/polym15193856.

13 C. Gutierrez Cisneros, H. Agten, E. Derveaux, P. Adriaensens, V. Bloemen and A. Mignon, Development Of A Biocompatible, Low-Cost Reinforcement Of Methacrylated Alginate Hydrogels Using Synthetic Crosslinking Agents, *React. Funct. Polym.*, 2025, **214**, 106330, DOI: 10.1016/j.reactfunctpolym.2025.106330.

14 V. Vállez-Gomis, S. Exojo-Trujillo, J. L. Benedé, A. Chisvert and A. Salvador, Stir Bar Sorptive-Dispersive Microextraction By A Poly(Methacrylic Acid-Co-Ethylene Glycol Dimethacrylate)-Based Magnetic Sorbent For The Determination Of Tricyclic Antidepressants And Their Main Active Metabolites In Human Urine, *Microchim. Acta*, 2022, **189**(2), 52, DOI: 10.1007/s00604-021-05156-7.

15 S. Briede, T. Biemans, O. Platnieks and S. Gaidukovs, Tailored Uv-Curable Acrylated Linseed Oil-Based Alkyds: Optimizing Crosslinking And Coating Performance Through Functionalization And Reactive Diluent Design, *Polymer*, 2025, **323**, 128227, DOI: 10.1016/j.polymer.2025.128227.

16 J. Wu, Y. Qian, C. A. Sutton, J. J. La Scala, D. C. Webster and M. P. Sibi, Bio-Based Furanic Di(Meth)Acrylates As Reactive Diluents For Uv Curable Coatings: Synthesis And Coating Evaluation, *ACS Sustain. Chem. Eng.*, 2021, **9**(46), 15537–15544, DOI: 10.1021/acssuschemeng.1c05588.

17 B. Eren, E. D. Karaçoban and B. Erdoğan, Synthesis And Characterization Of Scpuv/Scp-Curable Polyurethane Acrylates Derived From Trimethylolpropane And Hydroxyethyl Methacrylate: Effect Of 2-Hydroxyethyl Methacrylate Scp(Hema)/Scp Content On Thermal Stability, Gloss Properties, And Microstructure, *Polym. Eng. Sci.*, 2024, **65**(1), 327–337, DOI: 10.1002/pen.27012.

18 J. Yang, X. Liang, F. Liu, Y. Biao and J. He, Comparing Properties Of Urethane Dimethacrylate (Udma) Based 3D Printing Resin Using N-Acryloylmorpholine (Acmo) And Triethylene Glycol Dimethacrylate (Tegdma) Separately As Diluents, *J. Macromol. Sci., Part B*, 2024, **64**(9), 1005–1021, DOI: 10.1080/00222348.2024.2377507.

19 J. H. Vergara, S. K. Yadav, O. Bolarin, J. J. La Scala and G. R. Palmese, Synthesis And Characterization Of Low-Viscosity Bio-Based Styrene Alternatives For Bisphenol A Vinyl Ester Thermosetting Resins, *ACS Sustain. Chem. Eng.*, 2020, **8**(46), 17234–17244, DOI: 10.1021/acssuschemeng.0c06074.

20 Reactive Diluents Market Size & Share Analysis – Growth Trends & Forecasts, 2025 – 2030, Mordor Intelligence Homepage, https://www.mordorintelligence.com/industry-reports/reactive-diluents-market, accessed November 2025.

21 D. N. Lastovickova, F. R. Toulan, J. R. Mitchell, D. VanOosten, A. M. Clay, J. F. Stanzione, G. R. Palmese and J. J. La Scala, Resin, Cure, And Polymer Properties Of Photopolymerizable Resins Containing Scpbio-Derived/Scp Isosorbide, *J. Appl. Polym. Sci.*, 2021, **138**(25), app50574, DOI: 10.1002/app.50574.

22 O. Llorente, A. Barquero, M. Paulis and J. R. Leiza, Challenges To Incorporate High Contents Of Bio-Based Isobornyl Methacrylate (Iboma) Into Waterborne Coatings, *Prog. Org. Coat.*, 2022, **172**, 107137, DOI: 10.1016/j.porgcoat.2022.107137.

23 S. Malburet, H. Bertrand, C. Richard, C. Lacabanne, E. Dantras and A. Graillot, Biobased Epoxy Reactive Diluents Prepared From Monophenol Derivatives: Effect On Viscosity And Glass Transition Temperature Of Epoxy Resins, *RSC Adv.*, 2023, **13**(22), 15099–15106, DOI: 10.1039/d3ra01039b.

24 A. Kowalewska and K. Majewska-Smolarek, Eugenol-Based Polymeric Materials—Antibacterial Activity And Applications, *Antibiotics*, 2023, **12**(11), 1570, DOI: 10.3390/antibiotics12111570.

25 X. Fei, J. Wang, J. Zhu, X. Wang and X. Liu, Biobased Poly(Ethylene 2,5-Furancoate): No Longer An Alternative, But An Irreplaceable Polyester In The Polymer Industry, *ACS Sustain. Chem. Eng.*, 2020, **8**(23), 8471–8485, DOI: 10.1021/acssuschemeng.0c01862.

26 P. Voigt, N. Kiriy, K. Jähnichen and B. Voit, Application Of Biobased Monomers In Two-Component Methacrylate Resins Using Reaction Monitoring And Design-Of-Experiment Analysis, *ACS Sustain. Chem. Eng.*, 2024, **12**(5), 1984–1996, DOI: 10.1021/acssuschemeng.3c06446.

27 Q. He, L. Hu, Y. Huang, T. Huang, Z. Zhu, Y. Li, Y. Hu and Z. Yang, Eugenol-Based Multi-Functional Monomer As Reactive Diluent For High Bio-Content Uv-Curable Coatings, *Prog. Org. Coat.*, 2025, **200**, 109079, DOI: 10.1016/j.porgcoat.2025.109079.

28 J. S. Terry and A. C. Taylor, The Properties And Suitability Of Commercial Bio-Based Epoxies For Use In Fiber-Reinforced Composites, *J. Appl. Polym. Sci.*, 2021, **138**(20), 50417, DOI: 10.1002/app.50417.

29 F. Wang, D. Allen, S. Tian, E. Oler, V. Gautam, R. Greiner, T. O. Metz and D. S. Wishart, Cfm-Id 4.0 – A Web Server For Accurate Ms-Based Metabolite Identification, *Nucleic Acids Res.*, 2022, **50**(W1), W165–W174, DOI: 10.1093/nar/gkac383.

30 W. Liu, T. Xie and R. Qiu, Biobased Thermosets Prepared From Rigid Isosorbide And Flexible Soybean Oil Derivatives, *ACS Sustain. Chem. Eng.*, 2016, **5**(1), 774–783, DOI: 10.1021/acssuschemeng.6b02117.

31 C. Zhang, S. A. Madbouly and M. R. Kessler, Biobased Polyurethanes Prepared From Different Vegetable Oils, *ACS Appl. Mater. Interfaces*, 2015, **7**(2), 1226–1233, DOI: 10.1021/am5071333.

32 B. Kumar, S. Adil and J. Kim, Biomass-Derived Epoxy Resin And Its Application For High-Performance Natural Fiber Composites, *J. Reinf. Plast. Compos.*, 2024, 07316844241275225, DOI: 10.1177/07316844241275225.

33 Y. Liu, M.-Y. Liu, X.-G. Fan, L. Wang, J.-Y. Liang, X.-Y. Jin, R.-J. Che, W.-Y. Ying and S.-P. Chen, Four-Dimensional Printing Of Multifunctional Photocurable Resin Based On Waste Cooking Oil, *ACS Sustain. Chem. Eng.*, 2022, **10**(49), 16344–16358, DOI: 10.1021/acssuschemeng.2c05514.

34 Q. Wang, J. Thomas and M. D. Soucek, Investigation Of Uv-Curable Alkyd Coating Properties, *J. Coat. Technol. Res.*, 2023, **20**(2), 545–557, DOI: 10.1007/s11998-022-00697-9.

35 Y. Wu, P. A. Advincula, O. Giraldo-Londoño, Y. Yu, Y. Xie, Z. Chen, G. Huang, J. M. Tour and J. Lin, Sustainable 3D Printing Of Recyclable Biocomposite Empowered By Flash

Graphene, *ACS Nano*, 2022, **16**(10), 17326–17335, DOI: 10.1021/acsnano.2c08157.

36 D. Popescu, R. Hoogenboom, H. Keul and M. Moeller, Hydroxy Functional Acrylate And Methacrylate Monomers Prepared Via Lipase—Catalyzed Transacylation Reactions, *J. Mol. Catal. B: Enzym.*, 2010, **62**(1), 80–89, DOI: 10.1016/j.molcatb.2009.09.008.

37 K. Abida and A. Ali, Quantification Of Triacetin In A Mixture Of Tri-, Di-, Monoacetin And Glycerol By Qhnmr Technique, *J. Anal. Chem.*, 2023, **78**(4), 480–487, DOI: 10.1134/s1061934823040032.

38 L. Cseri, S. Kumar, P. Palchuber and G. Szekely, Nmr Chemical Shifts Of Emerging Green Solvents, Acids, And Bases For Facile Trace Impurity Analysis, *ACS Sustain. Chem. Eng.*, 2023, **11**(14), 5696–5725, DOI: 10.1021/acssuschemeng.3c00244.

39 Z. Grigale-Soročina, E. Vindedze, J. Kozela and I. Birks, Evaluation Of Reactive Diluent Impact On Stability Of Systems Viscosity In Uv-Curable Compositions, *Solid State Phenom.*, 2021, **320**, 150–154, DOI: 10.4028/www.scientific.net/ssp.320.150.

40 P. Rade, S. Swami, V. Pawane, R. Hawaldar, V. Giramkar, S. Joseph and B. Kale, Effect Of Functionality Of Diluents On Digital Light Processing (Dlp) Based Three-Dimensional (3D) Printing Of Uv-Curable Bisphenol A-Based Epoxy Acrylate Resin, *Polym. Eng. Sci.*, 2024, **64**(5), 2202–2213, DOI: 10.1002/pen.26686.

41 C. Ye, K. Janssen, G. H. M. Schnelting, V. S. D. Voet, R. Folkersma and K. Loos, Repairable 3D Printable Photopolymer Resins Based On Low-Activation-Energy Adaptable Covalent Bonding, *Polymer*, 2025, **319**, 127997, DOI: 10.1016/j.polymer.2024.127997.

42 T. Yuan, L. Zhang, T. Li, R. Tu and H. A. Sodano, 3D Printing Of A Self-Healing, High Strength, And Reprocessable Thermoset, *Polym. Chem.*, 2020, **11**(40), 6441–6452, DOI: 10.1039/d0py00819b.

43 Q. Wu, Y. Hu, J. Tang, J. Zhang, C. Wang, Q. Shang, G. Feng, C. Liu, Y. Zhou and W. Lei, High-Performance Soybean-Oil-Based Epoxy Acrylate Resins: "Green" Synthesis And Application In Uv-Curable Coatings, *ACS Sustain. Chem. Eng.*, 2018, **6**(7), 8340–8349, DOI: 10.1021/acssuschemeng.8b00388.

44 S. H. Liu, X. Q. Zhang, J. H. Liu, C. H. Lei and Z. X. Dong, A Novel Bio-Based Epoxy Resin From Oligomer: Excellent Processability, High Heat Resistance, And Intrinsic Flame Retardancy, *Express Polym. Lett.*, 2021, **15**(12), 1189–1205, DOI: 10.3144/expresspolymlett.2021.95.

45 Y. Hu, Q. Shang, J. Tang, C. Wang, F. Zhang, P. Jia, G. Feng, Q. Wu, C. Liu, L. Hu, W. Lei and Y. Zhou, Use Of Cardanol-Based Acrylate As Reactive Diluent In Uv-Curable Castor Oil-Based Polyurethane Acrylate Resins, *Ind. Crops Prod.*, 2018, **117**, 295–302, DOI: 10.1016/j.indcrop.2018.02.053.

46 W. Hua, Q. Lin, B. Qu, Y. Zheng, X. Liu, W. Li, X. Zhao, S. Chen and D. Zhuo, Exceptional Mechanical Properties And Heat Resistance Of Photocurable Bismaleimide Ink For 3D Printing, *Materials*, 2021, **14**(7), 1708, DOI: 10.3390/ma14071708.

47 Z. Wan, H. Zhang, M. Niu, W. Zhang, Y. Guo and H. Li, Development Of Lignin-Derived Uv-Curable Resin For Dlp 3D Printing, *Ind. Crops Prod.*, 2024, **221**, 119243, DOI: 10.1016/j.indcrop.2024.119243.

48 G. I. dos Santos, C. Gaglieri, R. T. Alarcon, A. de Moura, F. B. dos Santos and G. Bannach, Glycerol And Maleic Anhydride-Based Acrylic Polyester: A Solution For Greener Photocurable Resins For 3D Printing Of Renewable Materials, *ACS Sustain. Chem. Eng.*, 2025, **13**(25), 9771–9782, DOI: 10.1021/acssuschemeng.5c03006.

49 M. Shah, A. Ullah, K. Azher, Ur R. Asif, W. Juan, N. Aktürk, C. S. Tüfekci and M. U. Salamcı, Vat Photopolymerization-Based 3D Printing Of Polymer Nanocomposites: Current Trends And Applications, *RSC Adv.*, 2023, **13**(2), 1456–1496, DOI: 10.1039/d2ra06522c.

50 Y. Hu, Q. Shang, C. Wang, G. Feng, C. Liu, F. Xu and Y. Zhou, Renewable Epoxidized Cardanol-Based Acrylate As A Reactive Diluent For Uv-Curable Resins, *Polym. Adv. Technol.*, 2018, **29**(6), 1852–1860, DOI: 10.1002/pat.4294.

51 S. Briede, O. Platnieks, M. Dārziņa, A. Jirgensons and S. Gaidukovs, Effect Of Novel Furan-Based Ester Reactive Diluent On Structure And Properties Of Scpuv/Scp-Crosslinked Acrylated Rapeseed Oil, *J. Polym. Sci.*, 2023, **61**(24), 3318–3328, DOI: 10.1002/pol.20230451.

52 Z. Yang, J. Shan, Y. Huang, X. Dong, W. Zheng, Y. Jin and W. Zhou, Preparation And Mechanism Of Free-Radical/Cationic Hybrid Photosensitive Resin With High Tensile Strength For Three-Dimensional Printing Applications, *J. Appl. Polym. Sci.*, 2020, **138**(8), 49881–49891, DOI: 10.1002/app.49881.

53 Y. Cui, J. Yang, D. Lei and J. Su, 3D Printing Of A Dual-Curing Resin With Cationic Curable Vegetable Oil, *Ind. Eng. Chem. Res.*, 2020, **59**(25), 11381–11388, DOI: 10.1021/acs.iecr.0c01507.

54 H. Wang, Y. Wan, Q. Liu, X. Xie, K. Zhu, Q. Jiang, Y. Feng, P. Xiao, Z. Xiang, Q. Zhang, Y. Fan, X. Wu, Y. Zhu and R. Song, Association Between Urinary 2-Hydroxyethyl Mercapturic Acid And Dyslexia Among School-Aged Children, *Environ. Sci. Pollut. Res.*, 2023, **30**(45), 101091–101098, DOI: 10.1007/s11356-023-29418-4.

55 M. Kury, K. Ehrmann, G. A. Harakály, C. Gorsche and R. Liska, Low Volatile Monofunctional Reactive Diluents For Radiation Curable Formulations, *J. Polym. Sci.*, 2021, **59**(19), 2154–2169, DOI: 10.1002/pol.20210171.

56 E. Krumins, C. L. Joachim, B. Sutcliffe, A. Sohaib, L. J. Philippa, B. Brugnoli, C. C. Valentina, R. Cavanagh, R. Owen, C. Moloney, L. Ruiz-Cantu, I. Francolini, M. H. Steven, M. Shusteff, F. R. A. J. Rose, R. D. Wildman, Y. He and V. Taresco, Glycerol-Based Sustainably Sourced Resin For Volumetric Printing, *Green Chem.*, 2024, **26**(3), 1345–1355, DOI: 10.1039/d3gc03607c.

57 K. George, E. Krumins, E. Tan, Y. He, D. W. Ricky, R. Owen, J. Segal, C. C. Valentina and V. Taresco, Polyglycerol Resin Towards Sustainable 3D-Printing, *Faraday Discuss.*, 2026, **262**, 123–137, DOI: 10.1039/d5fd00043b.

58 G. Iago dos Santos, C. Gaglieri, R. T. Alarcon, A. de Moura, F. de. P. Alves dos Santos and G. Bannach, Glycerol And

Maleic Anhydride-Based Acrylic Polyester: A Solution For Greener Photocurable Resins For 3D Printing Of Renewable Materials, *ACS Sustain. Chem. Eng.*, 2025, **13**(25), 9771–9782, DOI: 10.1021/acssuschemeng.5c03006.

59 R. Ravotti, O. Fellmann, N. Lardon, L. Fischer, A. Stamatiou and J. Worlitschek, Synthesis And Investigation Of Thermal Properties Of Highly Pure Carboxylic Fatty Esters To Be Used As Pcm, *Appl. Sci.*, 2018, **8**(7), 1069, DOI: 10.3390/app8071069.